

Data-based modelling of low-order modes for AO control: what do on-sky experiments tell us?

Baptiste Sinquin¹, Caroline Kulcsár¹, Léonard Prengère¹², Henri-François Raynaud¹, Eric Gendron³, James Osborn⁴, Ali G. Basden⁴, Jean-Marc Conan², Nazim Bharmal⁴, Lisa Bardou⁴, Lazar Staykov⁴, Tim Morris⁴, Tristan Buey⁵, Fanny Chemla⁵, Matthieu Cohen⁵

¹Laboratoire Charles Fabry, Institut d'Optique Graduate School - CNRS, Palaiseau, France

²ONERA, The French Aerospace Lab, Châtillon, France

³Laboratoire d'Etudes Spatiales et d'Instrumentation en Astrophysique, Observatoire de Paris, Meudon, France

⁴Centre for Advanced Instrumentation, Durham University, South Road, Durham, United Kingdom

⁵Galaxies Etoiles Planètes et Instrumentation, Observatoire de Paris, Meudon, France



Adaptive optics for astronomy

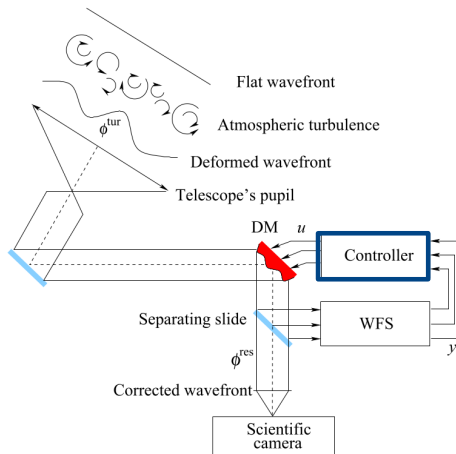


Figure 1: AO system schematics

I. SCAO on CANARY

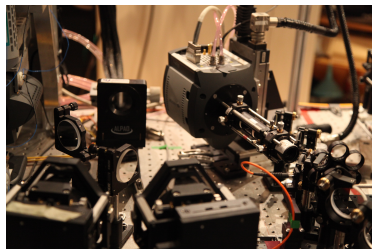
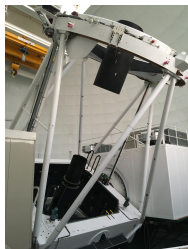
II. Disturbance model and the Linear-Quadratic-Gaussian (LQG) regulator

III. On-sky experiments

Case 1: large wind speed

Case 2: low wind speed

IV. Performance analysis



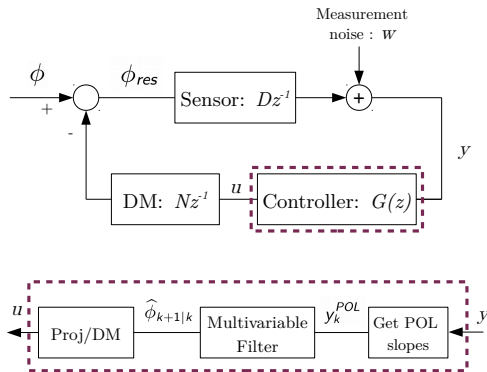
Run from July 18th to 22nd, 2019

	William Herschel
Telescope	
Diameter of prime mirror [m]	4.2
Central obscuration [m]	1.2
Shack-Hartmann	14×14
DM	15×15
Coupling	0.45
Control frequency [Hz]	200
Delay in the loop	2.25 frames

Seeing and wind profiles available in real-time ¹.

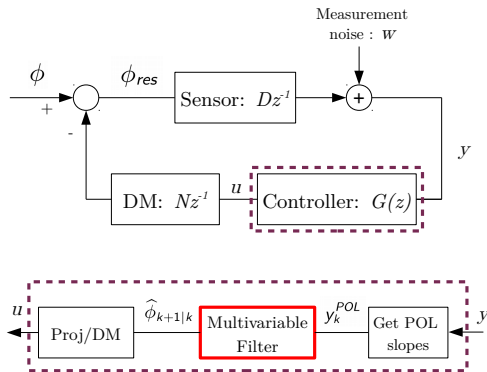
¹J. Osborn, "Characterising atmospheric turbulence using SCIDAR techniques," Imaging and Applied Optics 2018.

The LQG regulator



1. Minimum variance prediction of the wavefront, $\hat{\phi}_{k+1|k}$
2. Projection on the mirror's actuators, $u_k = M_{com} D \hat{\phi}_{k+1|k}$

The LQG regulator

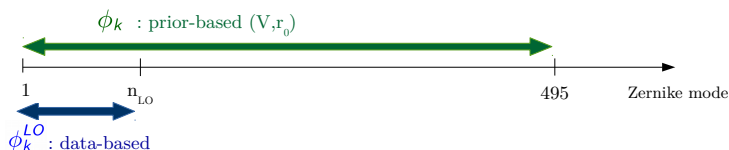


1. Minimum variance prediction of the wavefront, $\hat{\phi}_{k+1|k}$
2. Projection on the mirror's actuators, $u_k = M_{com} D \hat{\phi}_{k+1|k}$

Stochastic disturbance model

Wavefront expressed in a Zernike basis with 495 modes.

Total disturbance: $\phi_k + \phi_k^{LO}$



Prior-based model² (all modes):

$$\phi_{k+1} = A_1 \phi_k + A_2 \phi_{k-1} + v_k \quad (1)$$

Data-driven model (for the first n_{LO} modes):

$$\begin{cases} x_{k+1}^{LO} = A^{LO} x_k^{LO} + v_k \\ \phi_k^{LO} = C^{LO} x_k^{LO} + \eta_k \end{cases} \quad (2)$$

²G. Sivo, et al., "First on-sky SCAO validation of full LQG control with vibration mitigation on the CANARY pathfinder," Opt. Express 22, 23565-23591 (2014)

Stochastic disturbance model

y_k^{OL} : wavefront sensor measurement in open-loop

w_k : measurement noise

v_k : process noise

Concatenating prior-based and data-based models in state-space form:

$$\left\{ \begin{array}{l} \begin{bmatrix} \phi_{k+1} \\ \phi_k \\ x_{k+1}^{LO} \end{bmatrix} = \underbrace{\begin{bmatrix} A_1 & A_2 & 0 \\ I & 0 & 0 \\ 0 & 0 & A_{LO} \end{bmatrix}}_A \begin{bmatrix} \phi_k \\ \phi_{k-1} \\ x_k^{LO} \end{bmatrix} + v_k \\ \\ y_k^{OL} = \underbrace{\begin{bmatrix} 0 & D & D_{LO} \end{bmatrix}}_C \begin{bmatrix} \phi_k \\ \phi_{k-1} \\ x_k^{LO} \end{bmatrix} + w_k \end{array} \right. \quad (3)$$

Stochastic disturbance model

y_k^{OL} : wavefront sensor measurement in open-loop

w_k : measurement noise

v_k : process noise

Concatenating prior-based and data-based models in state-space form:

$$\left\{ \begin{array}{l} \begin{bmatrix} \phi_{k+1} \\ \phi_k \\ x_{k+1}^{LO} \end{bmatrix} = \underbrace{\begin{bmatrix} A_1 & A_2 & 0 \\ I & 0 & 0 \\ 0 & 0 & A_{LO} \end{bmatrix}}_A \begin{bmatrix} \phi_k \\ \phi_{k-1} \\ x_k^{LO} \end{bmatrix} + v_k \\ \\ y_k^{OL} = \underbrace{\begin{bmatrix} 0 & D & D_{LO} \end{bmatrix}}_C \begin{bmatrix} \phi_k \\ \phi_{k-1} \\ x_k^{LO} \end{bmatrix} + w_k \end{array} \right. \quad (3)$$

A linear multivariable filter:

$$\left\{ \begin{array}{l} x_{k+1} = Ax_k + v_k \\ y_k^{OL} = Cx_k + w_k \end{array} \right. \quad (4)$$

The LQG controller - minimum variance control

1. Minimum variance prediction of the wavefront, $\hat{\phi}_{k+1|k}$, with a Kalman filter:

$$\begin{cases} \hat{x}_{k+1|k} = (A - L_{\infty} C) \hat{x}_{k|k-1} + L_{\infty} y_k^{POL} \\ \hat{\phi}_{k+1|k} = C_{\phi} \hat{x}_{k+1|k} \end{cases} \quad (5)$$

2. Projection on the mirror inputs:

$$u_k = M_{com} D \hat{\phi}_{k+1|k} \quad (6)$$



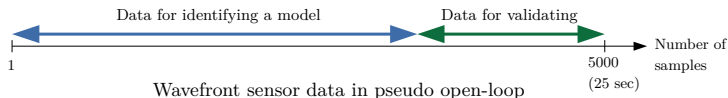
Model identification for the low-orders

Low-order disturbance model in state-space form,

$$\begin{cases} x_{k+1}^{LO} = A^{LO} x_k^{LO} + v_k \\ \phi_k^{LO} = C^{LO} x_k^{LO} + \eta_k \end{cases} \quad (7)$$

Now, estimate its matrices.

Model identification:

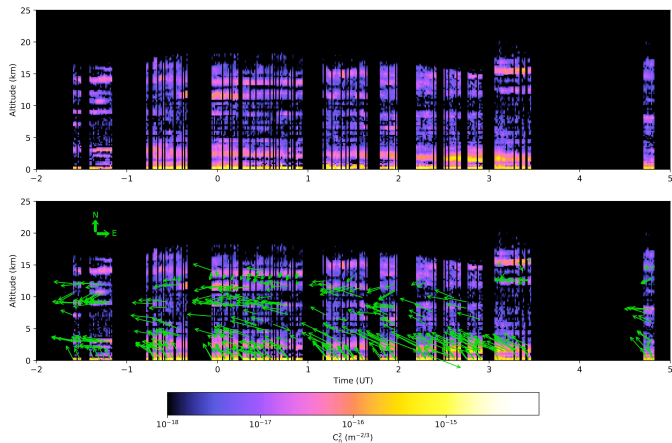


1. Static wavefront reconstruction (Maximum A Posteriori): $\phi^{LO} = R_{MAP} y^{OL}$
2. Apply the subspace algorithm N4SID³

³P. Van Overschee, B. De Moor, "N4SID: Subspace algorithms for the identification of combined deterministic-stochastic systems", Automatica, Vol. 30, no. 1, pp. 75–93, 1994.

Case 1: large wind speed (1/3) - the atmosphere

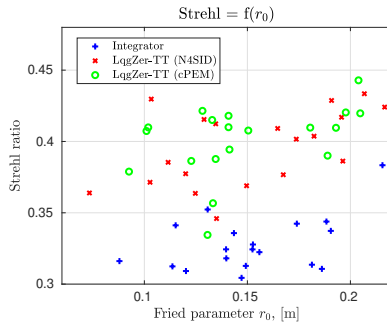
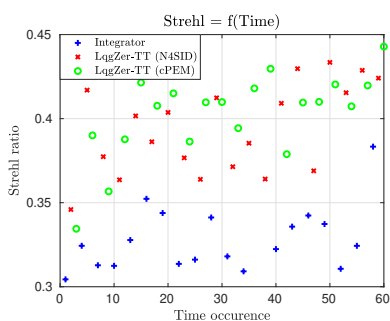
Evolution of the Cn^2 and windspeed from SLODAR



Length of the arrow in upper left position: 10m/s

Case 1: large wind speed (2/3) - on-sky results for $n_{LO} = 2$

Identification of tip and tilt dynamics either with N4SID, or cPEM (cascaded Prediction Error Method ⁴).

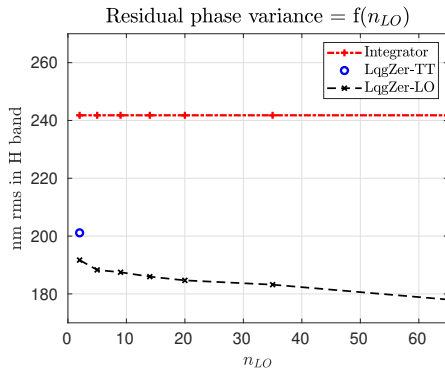


→ performance improves when identifying the tip-tilt dynamics from data.

→ cPEM slightly better than N4SID

⁴C. Kulcsár, P. Massioni, G. Sivo and H-F Raynaud, "Vibration mitigation in adaptive optics control," vol. 8447, Adaptive Optics Systems III SPIE, pp. 381 – 396, 2012

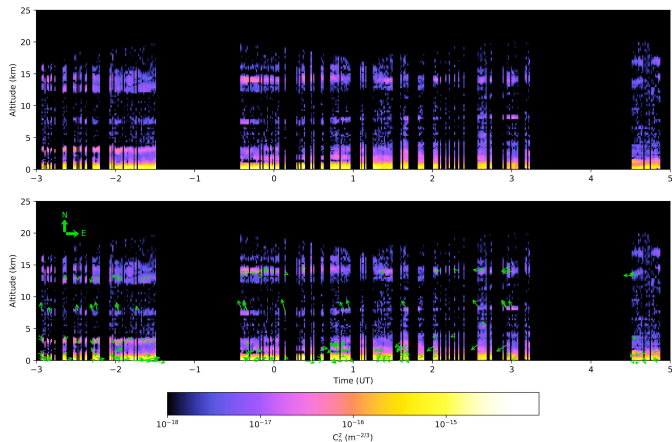
Case 1: large wind speed (2/2) - replay mode increasing n_{LO}



- lower residual variance with a minimum variance reconstruction of the tip and tilt
- the larger n_{LO} , the lower the residual phase variance

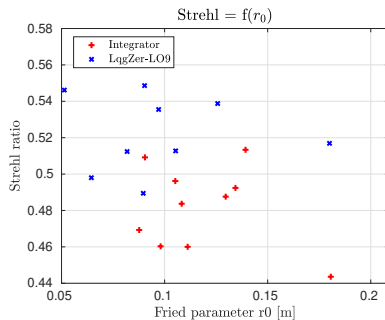
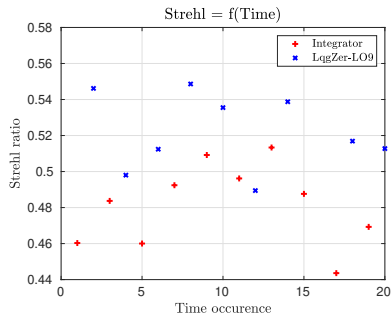
Case 2: low wind speed (1/4) - the atmosphere

Evolution of the Cn^2 and windspeed from SLODAR



Length of the arrow in upper left position: 10m/s

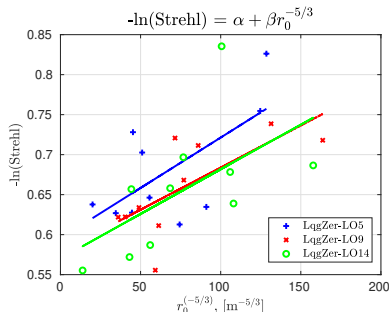
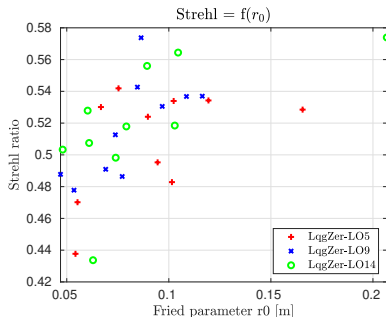
Case 2: low wind speed (2/4) - on-sky results with $n_{LO} = 9$



→ strong performance improvement when $n_{LO} = 9$

Case 2: low wind speed (3/4) - on-sky results for increasing n_{LO}

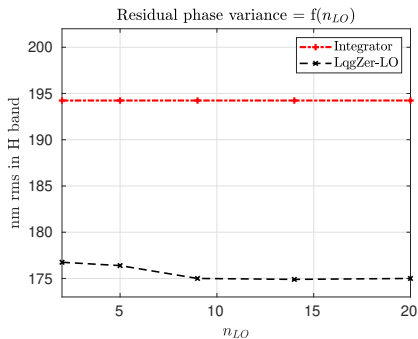
Maréchal approximation, $SR = e^{-\sigma_{res}^2}$
Showing trends via: $\sigma_{res}^2 \approx \alpha + \beta r_0^{-5/3}$



→ $n_{LO} = 9$ is better than $n_{LO} = 5$

→ $n_{LO} = 14$ does not improve significantly compared to $n_{LO} = 9$

Case 2: low wind speed (4/4) - replay mode



→ trends observed on-sky are confirmed in replay: data-driven model for 9 modes is most suitable

Performance analysis - rejection transfer functions

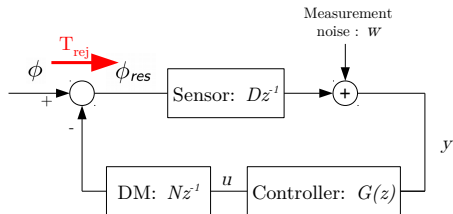
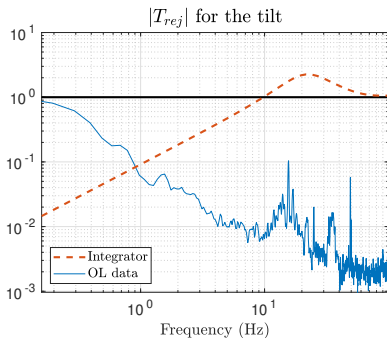
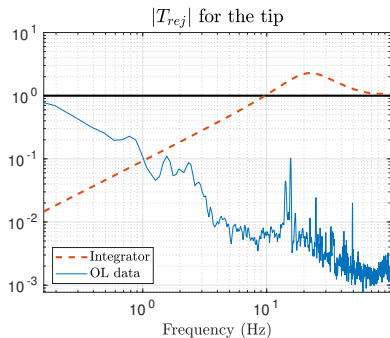


Figure 2: $\phi_{res} = T_{rej}\phi + T_{noise}w$



Performance analysis - rejection transfer functions

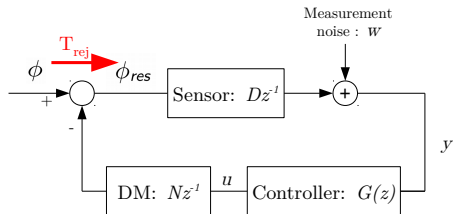
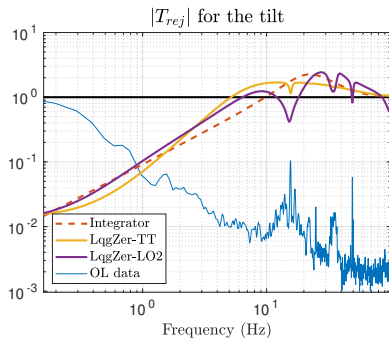
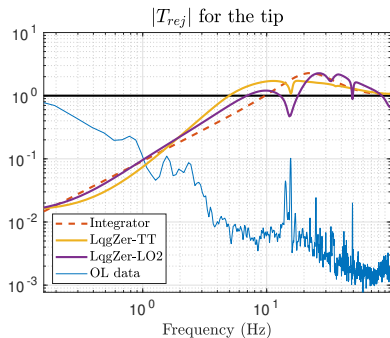


Figure 2: $\phi_{res} = T_{rej}\phi + T_{noise}w$



Performance analysis - rejection transfer functions

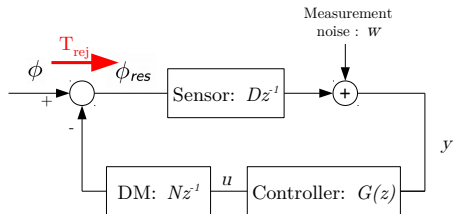
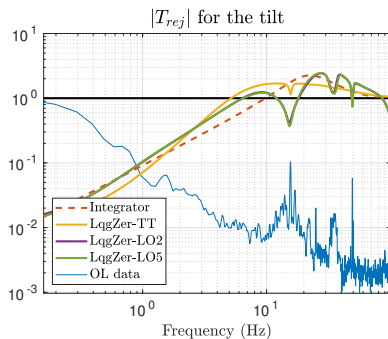
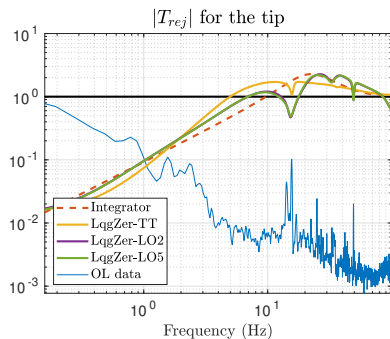
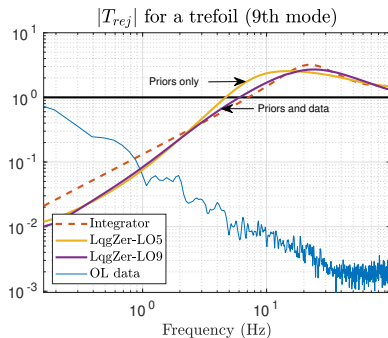
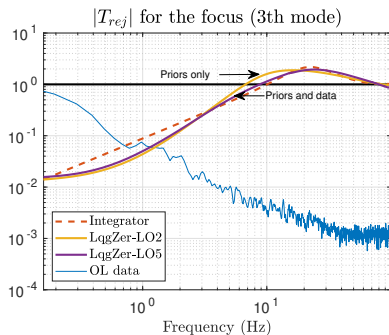


Figure 2: $\phi_{res} = T_{rej}\phi + T_{noise}w$



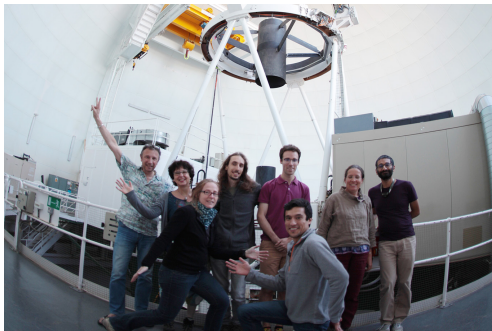
Performance analysis - rejection transfer functions



- better rejection for LQG at low frequencies, worse at high frequencies
- rejection from data better suited to the PSD of OL data

Conclusions from on-sky CANARY experiments at WHT

1. Identifying dynamics of more modes \rightarrow gain in performance even when without vibrations
2. Controller with 9 identified modes successfully used by other teams⁵⁶
3. Model-based control using wind profiles in tracking satellites (upcoming papers OSA AO + Optro2020)



⁵S. Haffert (Universiteit Leiden, NL) et al., "The multi-core integral-field unit (MCIFU): Overview and first light", under review for SPIE 2020.

⁶M. Langlois (CRAL-Lyon, France) al. "Mach-Zehnder Wavefront sensor for XAO: From laboratory tests to on sky measurements using the SCAO capability of CANARY at the William Herschel Telescope," under review for SPIE 2020.

Credit for the picture: Ali Bharmal